J-matrix calculation of electron-helium S-wave scattering. II. Beyond the frozen-core model

Dmitry A. Konovalov
ARC Centre for Antimatter-Matter Studies and
Discipline of Information Technology, School of Business,
James Cook University, Townsville, Queensland 4811, Australia

Dmitry V. Fursa and Igor Bray
ARC Centre for Antimatter-Matter Studies, Curtin University,
GPO Box U1987, Perth, Western Australia 6845, Australia
(Dated: August 30, 2012)

In the preceding J-matrix (JM) paper [D. A. Konovalov *et. al.* Phys. Rev. A **84**, 032707 (2011)], the S-wave e-He scattering (S-e-He) problem was solved within the frozen-core (FC) model of helium for impact energies in the range 0.1-1000eV. In this sequel, both target electrons are described within the configuration-interaction model of helium obtaining more accurate (compared to the FC model) first seven bound states of the S-wave helium. The presented JM calculations solve the S-e-He problem essentially exactly for the total elastic, $2^{1,3}S$, $3^{1,3}S$ excitation cross sections below the ionization threshold. The JM results are confirmed by the corresponding convergent-close-coupling (CCC) calculations creating a challenging benchmark for any current or future *ab initio* electron-atom scattering methods.

Above the ionization threshold, only the elastic and triplet excitation cross sections are obtained at the benchmark accuracy level. The total ionization and singlet excitation cross sections still exhibit noticeable pseudo-resonances (up to 10% fluctuations), which could not be eliminated with the considered number of target states (up to 95 eigenstates of He were considered).

PACS numbers: 34.80.Dp

I. INTRODUCTION

This study focuses on the S-wave e-He (S-e-He) scattering, where the target helium atom is in its ground state before the electron impact, and where only the partial wave with zero angular momentum ($l = 0$) is retained in all calculations and partial-wave expansions. The S-wave models have proven to be a very productive testing ground for *ab initio* scattering theories, see [1–18] for the S-wave e-H scattering (S-e-H) and [19–27] for the S-e-He problem. The main attraction of the S-wave models is that they retain most (arguably all) of the physics complexities of the full scattering problems while reduce the problems computationally. In particular, it is somewhat expected and implied that if a theoretical method solves a S-wave model, then the remaining partial waves could be solved with additional computational resources, which is indeed the case for the convergent-close-coupling (CCC) [28] and J-matrix (JM) [29, 30] methods.

The main goal of this study is to provide high accuracy total elastic and excitation S-e-He cross sections for 5-100eV impact energies highlighting resonant features of the cross sections. The need for such benchmark theoretical data is evident from the existing *ab initio* attempts to solve the S-e-He problem. Reviewing in reverse chronological order, in 2010 Bartlett and Stelbovics [25] developed a four-body propagating exterior scaling (PECS) method and reported results claiming to achieve "benchmark" level of accuracy. However none of their cross sections, including elastic and $2^{1,3}S$ excitation cross sections, displayed any resonances at the accuracy level achieved for the S-e-H problem [3]. In 2005, Horner et al. [24] reported results using time-dependent exterior complex scaling (TD-ECS), which also failed to described resonance behavior of the cross sections. In 2002 and 2004, the CCC method [21, 22] also did not examine the resonance regions with sufficiently fine energy grid. This is now corrected to some extent when in 2011 Konovalov et al. [27] reported the CCC and J-matrix (JM) *frozen-core* (FC) results clearly showing the resonances in the elastic and $n = 2$ (2^1S and 2^3S) excitation cross sections. And finally, the R-matrix method [31, 32] has never reported its results for the S-e-He problem.

The stated goal is attempted and achieved in many aspects by combining advantages of the CCC and JM methods, where the later has been recently revised [27] by merging it with the Fano's multi-configuration interaction matrix elements [33]. The CCC method is able to solve the scattering problem very accurately via the Lippmann-Schwinger equation [34]. However, it is not practical to run the CCC method for each of the many thousands of impact energy points required for the final benchmark results. On the other hand, the JM method is very efficient [35, 36] in calculating a vast number of energy points but numerical-convergence properties of the JM method remains largely unknown. The JM and CCC methods are implemented independently and use completely different approaches to solve the scattering equations. Therefore, the CCC and JM methods can be and were used to cross-verify that their results are conver-

gent within their own numerical parameters at key energy points.

The presented JM method is implemented using Java programming language, which is freely available for MS Windows, Mac OS, and many versions of Linux or Unix. See [37] for information on availability of the results and source code.

TABLE I: Energies and classifications for S-wave helium electron configurations. $\lambda_c = 4$, $\lambda_t = 1$, a.u.= 27.2116eV

Classification	threshold [eV]	Eigenvalues [a.u]	(N_c,N_t)
He($1s^2$,^1S)	0	-2.879 028 569 1	(50,50)
error =	0.001 80	-2.878 962 303	(7,30)
error =	0.177 47	-2.872 506 673	(1,30)
He($1s2s$,^3S)	19.178	-2.174 264 856 3	(50,50)
		-2.174 264 618	(7,30)
		-2.174 245 504	(1,30)
He($1s2s$,^1S)	19.996	-2.144 197 258 7	(50,50)
		-2.144 191 393	(7,30)
		-2.143 449 321	(1,30)
He($1s3s$,^3S)	22.056	-2.068 490 070	(7,30)
		-2.068 484 660	(1,30)
He($1s3s$,^1S)	22.266	-2.060 792 356	(7,30)
		-2.060 573 161	(1,30)
He($1s4s$,^3S)	22.928	-2.036 438 560	(7,30)
		-2.036 436 372	(1,30)
He($1s4s$,^1S)	23.011	-2.033 392 203	(7,30)
		-2.033 300 706	(1,30)
He($1s5s$,^3S)	23.305	-2.022 583 695	(7,30)
		-2.022 582 608	(1,30)
He($1s5s$,^1S)	23.346	-2.021 079 423	(7,30)
		-2.021 033 007	(1,30)
$He^+(1s)$	23.920	-2	

II. THEORY

Arguably, the main attraction of the JM method is its computational efficiency, where cross sections could be calculated many thousands of in one calculation.

Both JM and CCC methods rely on a

Let the nonorthogonal Laguerre functions used in the original JM method [35, 36] be referred to as the JM functions and denoted by $\{\xi_p(r)\}_{p=0}^{\infty}$,

$$\xi_p(r) = x^{l+1}\mathrm{e}^{-x/2}L_p^{2l+1}(x), \quad p = 0, 1, ..., \infty,$$

where $x = \lambda_{\mathrm{L}} r$, λ_{L} is the Laguerre exponential falloff, $l \equiv 0$ (for the S-model), and $L_p^{\alpha}(x)$ are the associated Laguerre polynomials [38]. The JM method splits the one-electron radial functional space into *inner* $\{\xi_p\}_{p=0}^{N-1}$ and *outer* $\{\xi_p\}_{p=N}^{\infty}$ subsets controlled by the number (N) of JM functions in the inner subset [35, 36].

III. RESULTS

A. Resonances in e-He S-wave scattering

[TODO] Atomic unit of energy (or Hartree) was set to 27.2116 eV. A tabular form of the JM and CCC cross sections is available from jmatrix.googlecode.com .

Again, both CCC and JM methods described the target helium atom , where the target eigenstates were constructed from the first N_t JM functions (**??**). Convergence in the CCC cross sections (Figs. **??** and **??**) was achieved at N_t =?, where the corresponding JM cross sections converged at N_t =? and N =?.

IV. CONCLUSIONS

Acknowledgments

This work was supported by the Australian Research Council. IB acknowledges the Australian National Computational Infrastructure Facility and its Western Australian node iVEC.

[1] A. Temkin, Phys. Rev. **126**, 130 (1962).
[2] E. J. Heller and H. A. Yamani, Phys. Rev. A **9**, 1209 (1974).
[3] R. Poet, J. Phys. B **11**, 3081 (1978).
[4] R. Poet, J. Phys. B **13**, 2995 (1980).
[5] R. Poet, J. Phys. B **14**, 91 (1981).
[6] J. Callaway and D. H. Oza, Phys. Rev. A **29**, 2416 (1984).
[7] I. Bray and A. T. Stelbovics, Phys. Rev. Lett. **69**, 53 (1992).
[8] A. K. Bhatia, B. I. Schneider, and A. Temkin, Phys. Rev. Lett. **70**, 1936 (1993).
[9] D. A. Konovalov and I. E. McCarthy, J. Phys. B **27**, L407 (1994).
[10] W. Ihra, M. Draeger, G. Handke, and H. Friedrich, Phys. Rev. A **52**, 3752 (1995).
[11] M. S. Pindzola and D. R. Schultz, Phys. Rev. A **53**, 1525 (1996).
[12] S. Jones and A. T. Stelbovics, Phys. Rev. A **66**, 032717 (2002).
[13] S. Jones and A. T. Stelbovics, Phys. Rev. Lett. **84**, 1878 (2000).
[14] M. Baertschy, T. N. Rescigno, W. A. Isaacs, and C. W. McCurdy, Phys. Rev. A **60**, R13 (1999).
[15] A. T. Stelbovics, Phys. Rev. Lett. **83**, 1570 (1999).
[16] C. W. McCurdy, D. A. Horner, and T. N. Rescigno, Phys. Rev. A **65**, 042714 (2002).
[17] P. L. Bartlett and A. T. Stelbovics, Phys. Rev. A **69**, 022703 (2004).
[18] A. L. Frapiccini, J. M. Randazzo, G. Gasaneo, and F. D. Colavecchia, J. Phys. B **43**, 101001 (2010).

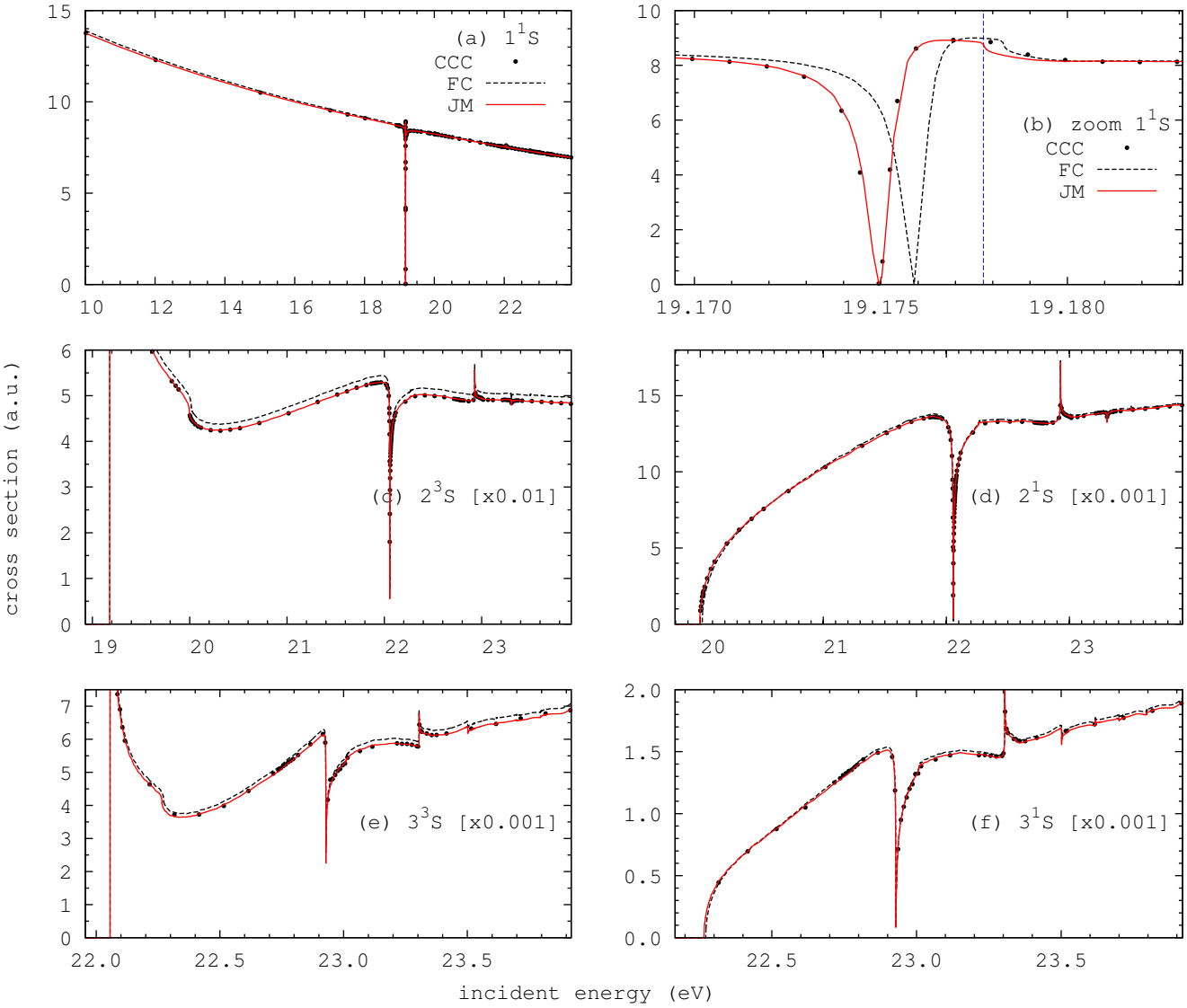

FIG. 1: (Color online) Elastic (1^1S), $n = 2$ (2^3S and 2^1S) and $n = 3$ (3^3S and 3^1S) single-excitation cross sections below the ionization threshold (23.92eV from Table I) for the e-He S-wave scattering model. Sub-figure (b) zooms in on the 2^3S excitation threshold (Table I) shown by the vertical dashed line. Frozen-core (FC), JM and CCC results were shifted by 0.17747eV, 0.0018eV and 0.0018eV (Table I), respectively.

[19] M. Draeger, G. Handke, W. Ihra, and H. Friedrich, Phys. Rev. A **50**, 3793 (1994).
[20] M. S. Pindzola, D. Mitnik, and F. Robicheaux, Phys. Rev. A **59**, 4390 (1999).
[21] C. Plottke, I. Bray, D. V. Fursa, and A. T. Stelbovics, Phys. Rev. A **65**, 032701 (2002).
[22] C. Plottke, P. Nicol, I. Bray, D. V. Fursa, and A. T. Stelbovics, J. Phys. B **37**, 3711 (2004).
[23] D. A. Horner, C. W. McCurdy, and T. N. Rescigno, Phys. Rev. A **71**, 010701(R) (2005).
[24] D. A. Horner, C. W. McCurdy, and T. N. Rescigno, Phys. Rev. A **71**, 012701 (2005).
[25] P. L. Bartlett and A. T. Stelbovics, Phys. Rev. A **81**, 022715 (2010).
[26] P. L. Bartlett and A. T. Stelbovics, Phys. Rev. A **81**, 022716 (2010).
[27] D. A. Konovalov, D. V. Fursa, and I. Bray, Phys. Rev. A **84**, 032707 (2011).
[28] D. V. Fursa and I. Bray, Phys. Rev. A **52**, 1279 (1995).
[29] D. A. Konovalov and I. E. McCarthy, J. Phys. B **27**, L741 (1994).
[30] D. A. Konovalov and I. E. McCarthy, J. Phys. B **28**, L139 (1995).
[31] W. C. Fon, K. P. Lim, K. Ratnavelu, and P. M. J. Sawey, Phys. Rev. A **50**, 4802 (1994).
[32] M. Stepanovic, M. Minic, D. Cvejanovic, J. Jureta, J. Kurepa, S. Cvejanovic, O. Zatsarinny, and K. Bartschat, J. Phys. B **39**, 1547 (2006).
[33] U. Fano, Phys. Rev. **140**, A67 (1965).
[34] I. Bray and A. T. Stelbovics, Phys. Rev. A **46**, 6995 (1992).
[35] E. J. Heller and H. A. Yamani, Phys. Rev. A **9**, 1201

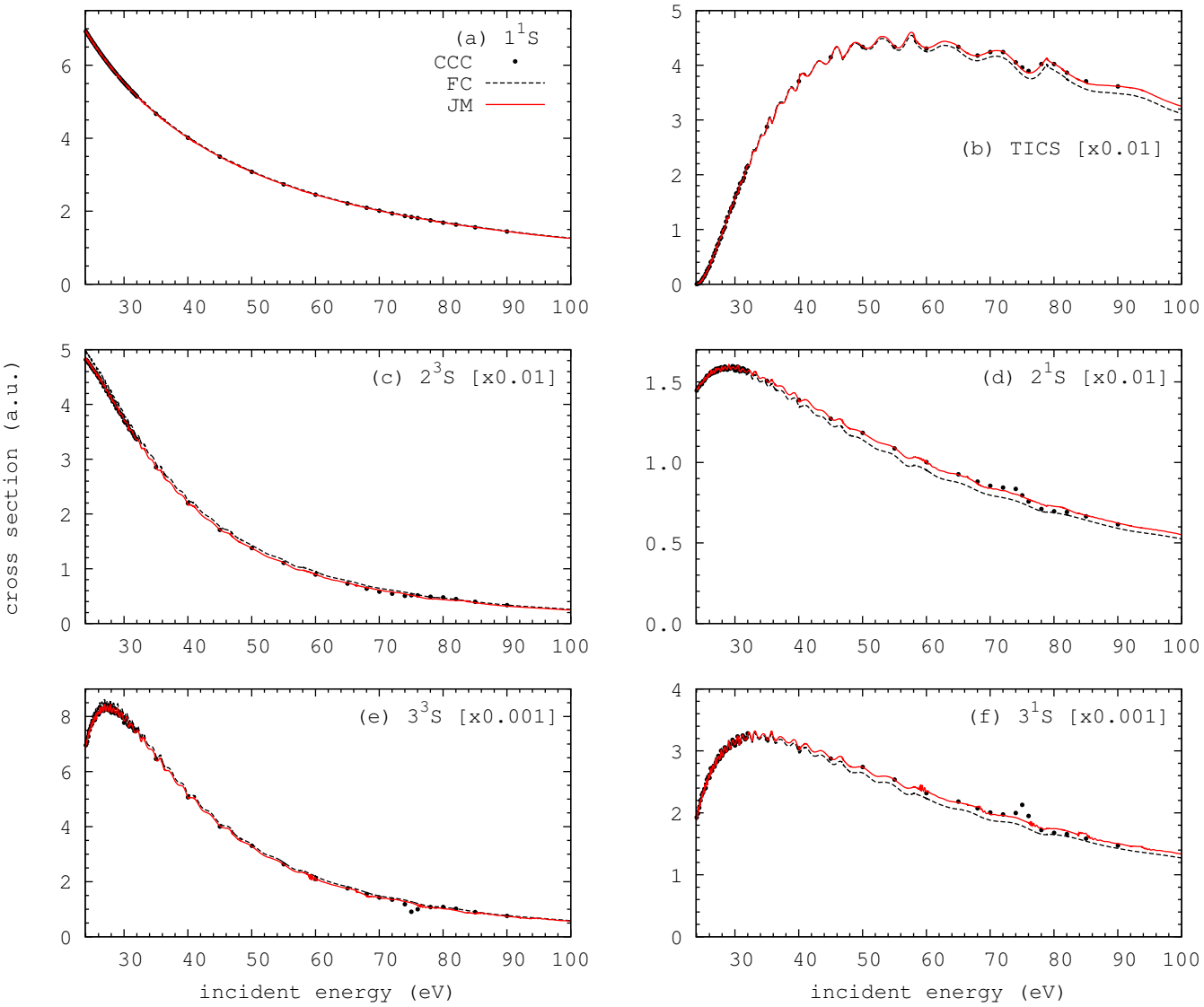

FIG. 2: (Color online) The same as in Fig. 1 but above the ionization threshold.

(1974).
[36] J. Broad and W. Reinhardt, J. Phys. B **9**, 1491 (1976).
[37] *The complete Java source code used in this study is freely available for academic use from jmatrix.googlecode.com or a relevant link at www.dmitrykonovalov.org . .*
[38] M. Abramowitz and I. A. Stegun, eds., *Handbook of Mathematical Functions* (Dover Publications, Mineola, NY, 1965).

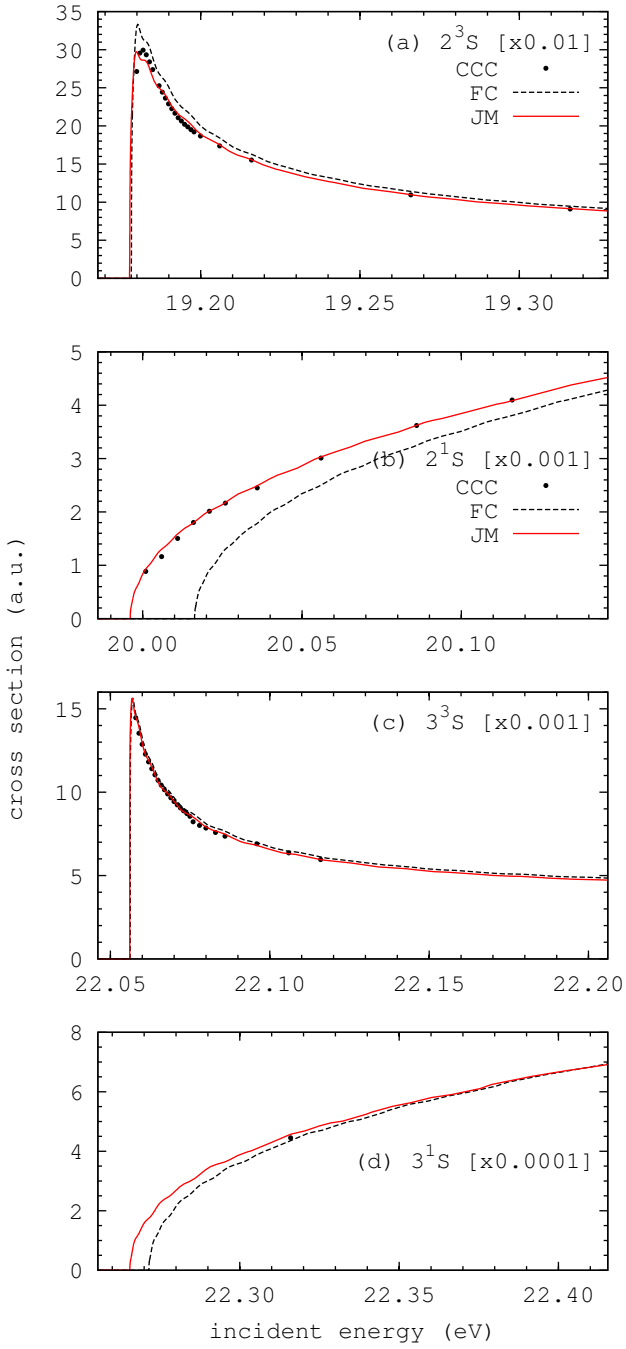

FIG. 3: (Color online) The same as in Fig. 1 but zooming in on the corresponding excitation threshold energies (Table I).

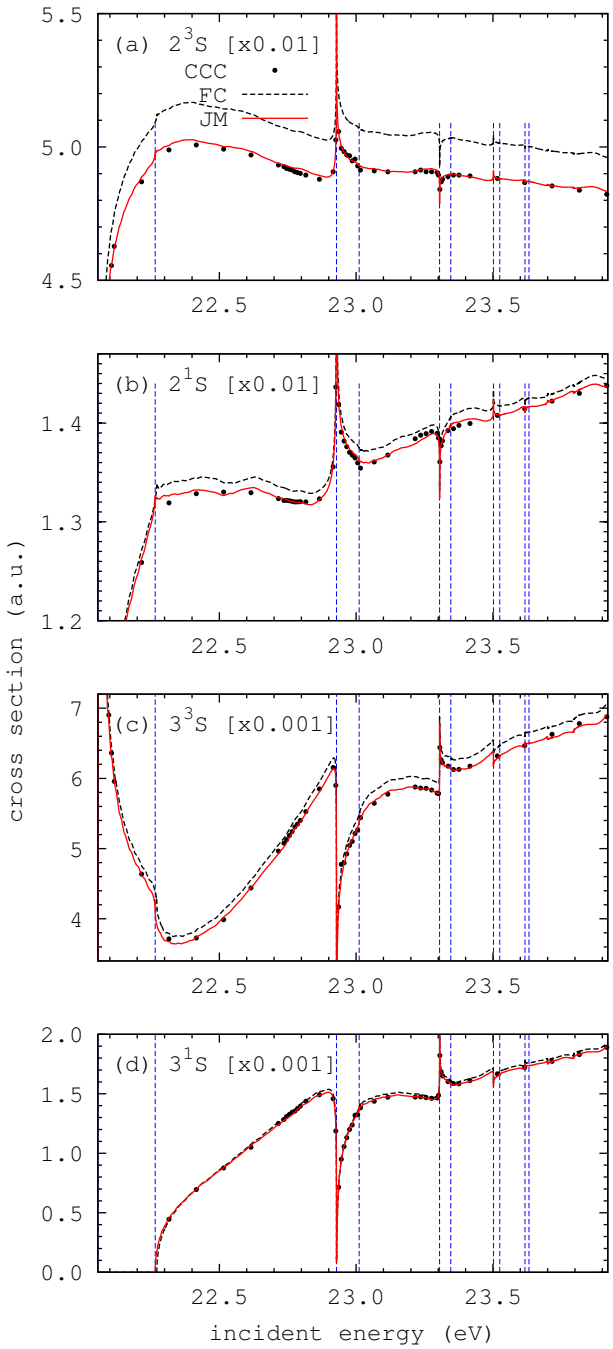

FIG. 4: (Color online) The same as in Fig. 1 but starting from the 3^3S threshold and aligned by incident energies. The 3^1S, $4^{3,1}S$, ..., $7^{3,1}S$, excitation thresholds (Table I) are shown by vertical dashed lines (from left to right).